SCIENTIFIC REPORTS

OPEN

SUBJECT AREAS:
BOSE-EINSTEIN CONDENSATES
THEORETICAL PHYSICS
FERROMAGNETISM
SURFACES, INTERFACES AND THIN FILMS

Received
10 December 2012

Accepted
15 February 2013

Published
4 March 2013

Correspondence and requests for materials should be addressed to W.M.S. (wsaslow@tamu.edu)

Phase Diagram for Magnon Condensate in Yttrium Iron Garnet Film

Fuxiang Li[1], Wayne M. Saslow[1] & Valery L. Pokrovsky[1,2]

[1]Dept. of Physics, Texas A&M University, College Station, TX 77843-4242, [2]Landau Institute for Theoretical Physics, Chernogolovka, Moscow District 142432, Russia.

Recently, magnons, which are quasiparticles describing the collective motion of spins, were found to undergo Bose-Einstein condensation (BEC) at room temperature in films of Yttrium Iron Garnet (YIG). Unlike other quasiparticle BEC systems, this system has a spectrum with two degenerate minima, which makes it possible for the system to have two condensates in momentum space. Recent Brillouin Light Scattering studies for a microwave-pumped YIG film of thickness $d = 5$ μm and field $H = 1$ kOe find a low-contrast interference pattern at the characteristic wavevector Q of the magnon energy minimum. In this report, we show that this modulation pattern can be quantitatively explained as due to unequal but coherent Bose-Einstein condensation of magnons into the two energy minima. Our theory predicts a transition from a high-contrast symmetric state to a low-contrast non-symmetric state on varying the d and H, and a new type of collective oscillation.

Bose-Einstein condensation (BEC), one of the most intriguing macroscopic quantum phenomena, has been observed in equilibrium systems of Bose atoms, like ^{4}He[1,2], ^{87}Rb[3] and ^{23}Na[4]. Recent experiments have extended the concept of BEC to non-equilibrium systems consisting of photons[5] and of quasiparticles, such as excitons[6], polaritons[7–9] and magnons[10,11]. Among these, BEC of magnons in films of Yttrium Iron Garnet (YIG), discovered by the group of Demokritov[11–17], is distinguished from other quasiparticle BEC systems by its room temperature transition and two-dimensional anisotropic properties. In particular, the spin-wave energy spectrum of a YIG film shows two energetically degenerate minima. Therefore it is possible that the system may have two condensates in momentum space[18]. An experiment by Nowik-Boltyk *et al.*[17] indeed shows a low-contrast spatial modulation pattern, indicating that there is interference between the two condensates. Current theories[19–24] do not describe the appearance of coherence or the distribution of the two condensates.

This report points out that a complete description of BEC in microwave-pumped YIG films must account for the 4th order interactions, including previously neglected magnon-non-conserving terms originating in the dipolar interactions. The theory explains not only the appearance of coherence but also quantitatively explains the low contrast of the experimentally observed interference pattern. Moreover, the theory predicts that, on increasing the film thickness from a small value d, there is a transition from a high-contrast symmetric state for $d < d_c$, with equal numbers of condensed magnons filling the two minimum states, to low-contrast coherent non-symmetric state for $d > d_c$, with different numbers of condensed magnons filling the two minimum states. In comparatively thin films ($d < 0.2$ μm) the same transition can be driven by an external magnetic field H. At another critical thickness $d^* > d_c$, the sum of phases of the two condensates changes from π to 0; at this transition point the system is in a completely non-symmetric state with only one condensate, for which there is no interference. In the experiment of Ref. 17 the thickness of film was larger than d^*. We suggest that the phase transitions may be identified by measuring the contrast of the spatial interference pattern for various d and H. We also predict a new type of collective magnetic oscillation in this system and discuss the possibility of domain walls in non-symmetric states.

Results

Phase diagram. We consider a YIG film of thickness d with in-plane magnetic field H (see inset of Fig. 1). The 4-th order interaction of condensate amplitudes reads[25–27]:

$$\hat{V}_4 = A\left[c_Q^\dagger c_Q^\dagger c_Q c_Q + c_{-Q}^\dagger c_{-Q}^\dagger c_{-Q} c_{-Q}\right] + 2B c_Q^\dagger c_{-Q}^\dagger c_{-Q} c_Q + C\left[c_Q^\dagger c_Q c_Q c_{-Q} + c_{-Q}^\dagger c_{-Q} c_{-Q} c_Q + h.c.\right]. \quad (1)$$

where, $c_{\pm Q}$ and $c_{\pm Q}^\dagger$ are the annihilation and creation operators for magnons in the two condensates located at the two energy minima $(0, \pm Q)$ in the 2-D momentum space (see. Fig. 1). The coefficients in Eq.(1) are:

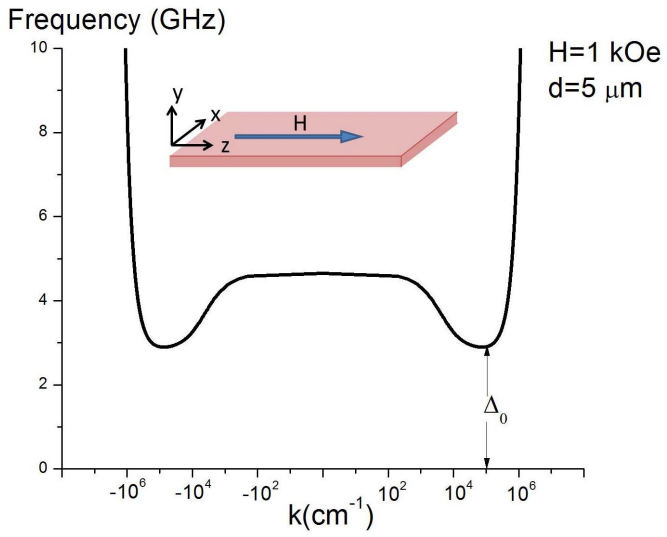

Figure 1 | The magnon spectrum in the k_z direction for $d = 5$ μm and $H = 1$ kOe. The inset is a schematic diagram of YIG film.

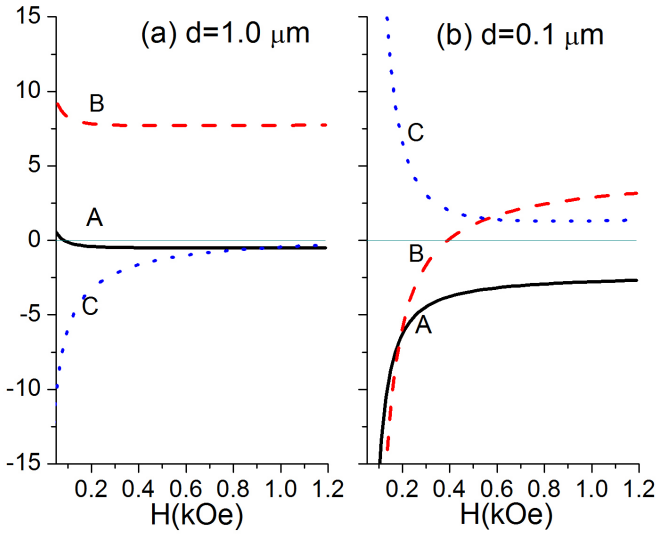

Figure 2 | The interaction coefficients A, B and C (in units of mK/N, with N the total number of spins in the film) as a function of magnetic field H for film thickness (a) $d = 1.0$ μm and (b) $d = 0.1$ μm.

$$A=-\frac{\hbar\omega_M}{4SN}[(\alpha_1-\alpha_3)F_Q-2\alpha_2(1-F_{2Q})]-\frac{DQ^2}{2SN}[\alpha_1-4\alpha_2],$$
$$B=\frac{\hbar\omega_M}{2SN}[(\alpha_1-\alpha_2)(1-F_{2Q})-(\alpha_1-\alpha_3)F_Q]+\frac{DQ^2}{SN}[\alpha_1-2\alpha_2], \quad (2)$$
$$C=\frac{\hbar\omega_M}{8SN}\left[\left(3\alpha_1-\frac{20}{3}\alpha_3+3\alpha_2\right)F_Q+\frac{16}{3}\alpha_3(1-F_{2Q})\right]+\frac{DQ^2}{SN}\alpha_3,$$

with $\alpha_1 = u^4 + 4u^2v^2 + v^4$, $\alpha_2 = 2u^2v^2$ and $\alpha_3 = 3uv(u^2 + v^2)$. Here, u and v are the coefficients of Bogoliubov transformation (see the Methods section for details). $S = 14.3$ is the effective spin, N the total number of spins in the film, M the magnetization and $\hbar\omega_M = \gamma 4\pi M$ with gyromagnetic ratio $\gamma = 1.2 \times 10^{-5}$ eV/kOe. D is proportional to the exchange constant and $F_k = (1 - e^{-kd})/kd$. Similar results for the coefficients A and B were obtained in Ref. 19. Coefficient C, which violates magnon number conservation, was not considered previously. Below we show that C is the only source of coherence between the two condensates. The three coefficients A, B and C, whose values as functions of H are shown in Fig. 2 for two typical values of d, determine the distribution of condensed magnons in the two degenerate minima. Ref. 19 assumed a symmetric state with condensed magnons in both minima having equal amplitudes and equal phases. Later, Ref. 20 assumed filling of only one minimum. More recently Ref. 24 considered Josephson-like oscillations by starting from two condensates with equal numbers of magnons but different phases. Our theory predicts coherent condensates and the ratio of their amplitudes without any additional assumptions.

In terms of condensate numbers $N_{\pm Q}$ and phases $\phi_\pm$, the condensate amplitudes are $c_{\pm Q} = \sqrt{N_{\pm Q}}e^{i\phi_\pm}$. Substituting them into eq.(1) we find:

$$V_4 = A\left(N_Q^2 + N_{-Q}^2\right) + 2BN_QN_{-Q} + 2C\cos\Phi\left(N_Q^{\frac{3}{2}}N_{-Q}^{\frac{1}{2}} + N_Q^{\frac{1}{2}}N_{-Q}^{\frac{3}{2}}\right), \quad (3)$$

where we introduce the total phase $\Phi = \phi_+ + \phi_-$. To minimize this energy, Φ must equal π for $C > 0$ and must equal 0 for $C < 0$. Fig. 2 shows that the sign of C changes for different d and H, which indicates a transition of Φ between 0 and π. For both $C > 0$ and $C < 0$ a coherence between the two condensate amplitudes is established. In contrast to the Josephson-like interaction, the sum rather than the difference of the two condensate phases is fixed.

Since the total number of condensed magnons $N_c = N_Q + N_{-Q}$ is uniquely determined by the pumping (see Methods), the energy is minimized only by the so far unspecified difference $\delta = N_Q - N_{-Q}$. In terms of N_c and δ the condensate energy eq.(3) is:

$$V_4 = \frac{1}{2}\left[(A+B)N_c^2 - (B-A)\delta^2 - 2|C|N_c\sqrt{N_c^2-\delta^2}\right]. \quad (4)$$

The ground state of the condensates depends on the criterion parameter:

$$\Delta = A - B + |C|. \quad (5)$$

When $\Delta > 0$, $\delta = 0$ minimizes the energy, so the two minima are filled with equal number of condensed magnons. This is the symmetric state with $N_Q = N_{-Q}$. When $\Delta < 0$, the minimum shifts to $\frac{\delta^2}{N_c^2} = 1 - \frac{C^2}{(B-A)^2}$. This is the non-symmetric state with $N_Q \neq N_{-Q}$. The transition from symmetric to non-symmetric state at $\Delta = 0$ is of the second order. There is no metastable state of these states. At $C = 0$ one finds $\delta = \pm N_c$, which corresponds to a completely non-symmetric state with only one condensate. The ground state of the non-symmetric state is doubly-degenerate, corresponding to the two possible signs for δ. Fig. 3 shows that for a film thickness of about 0.05 μm, the symmetric state is energy favorable up to $H = 1.2$ T. For $d = 0.08$ μm, on increasing H to about 0.6 kOe, there is a transition from symmetric to non-symmetric state. For a larger thickness $d = 0.1$ μm or $d = 1$ μm, the ground state is non-symmetric for $H > 0.3$ kOe.

Fig. 4 shows that the phase diagram in (d, H) space has three different regions, separated by two critical transition lines, $d_c(H)$ and $d^*(H)$, corresponding to $\Delta = 0$ and $C = 0$, respectively. For d=0.13−0.16 μm, the system possesses re-entrant behavior (NS $\Phi=\pi$, to NS Φ=0, to NS $\Phi=\pi$). As shown below, measurement of the contrast, or modulation depth[17], of the spatial interference pattern permits identification of the different condensate states.

Zero sound. In two-condensate states the relative phase $\delta\phi = \phi_+ - \phi_-$ is a Goldstone mode. Its oscillation, coupled with the oscillation of the number density $\delta n = n_Q - n_{-Q}$ represents a new type of collective excitation, which we call zero sound (as in Landau's Fermi liquid, this mode is driven by the self-consistent field rather than collisions). Solving a properly modified Gross-Pitaevskii

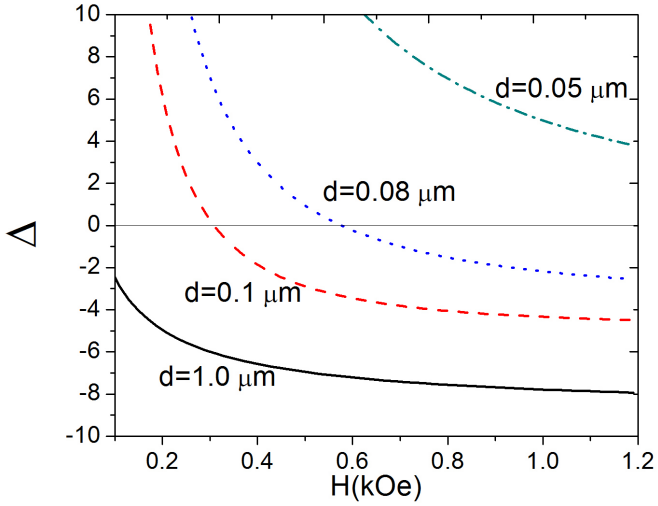

Figure 3 | The criterion of transition from non-symmetric to symmetric phase, Δ (in units of mK/N), as a function of magnetic field *H* for different values of thickness *d*.

equation (see Methods), we find its spectrum. In the symmetric state it is:

$$\omega = \sqrt{\frac{\hbar^2 k^4}{4m^2} + N_c \Delta \frac{k^2}{m}}. \qquad (6)$$

The magnon effective mass is of the order of the electron mass. The density of condensed magnons $n_c = N_c/V$ is about 10^{18} cm^{-3} and $\Delta \approx$ 10 mK/N. The sound speed for small k in this case is $v_{0s} = \sqrt{N_c \Delta / m}$, which is about 100 m/s. Near the transition point $\Delta = 0$, the velocity of this zero sound goes to zero. For the non-symmetric state, the spectrum is:

$$\omega = \sqrt{\frac{\hbar^2 k^4}{4m^2}\kappa + N_c (B-A)(\kappa - 1)\frac{k^2}{m}}, \qquad (7)$$

where $\kappa \equiv \frac{(B-A)^2}{C^2}$. In the experiment of Ref. 17, $\kappa \sim 10^4$ and $B - A$ = 8.4 mK/*N*. An estimate of the sound speed gives 3×10^3 m/s. The dispersions of zero sound for symmetric and non-symmetric states

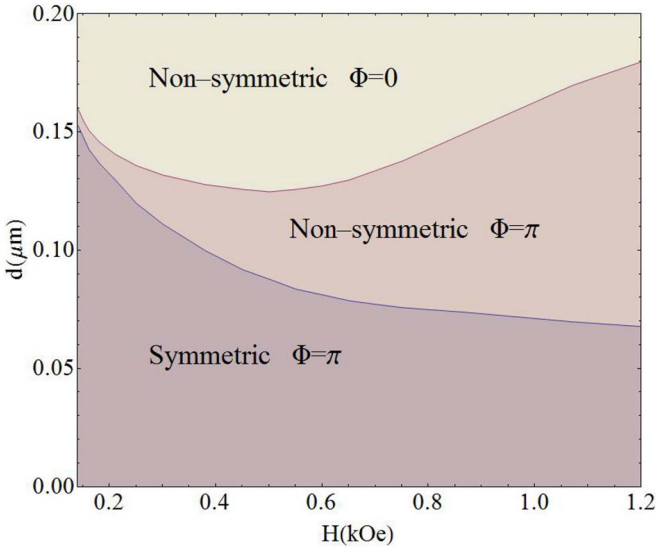

Figure 4 | The phase diagram for different values of thickness *d* and magnetic field *H*.

are shown in Fig. 5. Note that the range of applicability of the linear approximation strongly shrinks at small C since the density of one of the condensates becomes very small and the phase fluctuations grow.

Domain wall. Since the ground state of the non-symmetric state is doubly degenerate, it can consist of domains with different signs of δ separated by domain walls. The width w of a domain wall is of the order of $\sqrt{\frac{\hbar^2}{2mN_c|\Delta|}}$. For the data of Ref.17, $w \approx 10$ μm. The domain wall energy per unit area is $\approx 10^{-9}$ J/m^2.

Discussion

The ground state wave function $\Psi(z)$ generally is a superposition of two condensate amplitudes $\Psi(z) = (c_Q e^{iQz} + c_{-Q} e^{-iQz})/\sqrt{V}$, where $c_{\pm Q} = \sqrt{N_{\pm Q}} e^{i\phi_\pm}$ and V is the volume of the film. The spatial structure of $\Psi(z)$ can be measured by Brillouin Light Scattering (BLS). The BLS intensity is proportional to the condensate density $|\Psi|^2 = n_Q + n_{-Q} + 2\sqrt{n_Q n_{-Q}}\cos(2Qz + \phi_+ - \phi_-)$.

In their recent experiment, Nowik-Boltyk *el al*[17] observed the interference pattern associated with the ground state. They found that the contrast of this periodic spatial modulation is far below 100%; of the order 3%. The present theory can quantitatively explain this result. In the experiment of Ref. 17, d = 5.1 μm and H = 1 kOe, eq.(2) for A, B and C then gives $A = -0.168$ mK/*N*, $B = 8.218$ mK/*N* and $C = -0.203$ mK/*N*, so $\Delta < 0$. This corresponds to the non-symmetric state, where the ratio of the numbers of magnons in the two condensates is $\frac{N_{-Q}}{N_Q} \approx \frac{C^2}{4(B-A)^2}$ (assume $\delta > 0$). The contrast is $\beta = \frac{|\Psi|^2_{max} - |\Psi|^2_{min}}{|\Psi|^2_{max} + |\Psi|^2_{min}}$. Since $C \ll B$ and $N_{-Q} \ll N_Q$, $\beta \approx 2\sqrt{\frac{N_{-Q}}{N_Q}} \approx \frac{|C|}{|B-A|}$. For the above values of A, B and C, β is of order 2.4%, in good agreement with experiment. The smallness of C (and A) in comparison to B is associated with a large parameter d/l where $l = \sqrt{\frac{D}{\pi\gamma M}}$ is an intrinsic length scale of the system and $l \sim 10^{-6}$ m. In terms of this parameter, $\frac{|C|}{B} \sim \left(\frac{l}{d}\right)^{2/3}$.

Experimentally[17] the contrast β reaches the saturation value at a comparatively small pumping power, corresponding to the appearance of BEC. This agrees with our expression for β, which depends

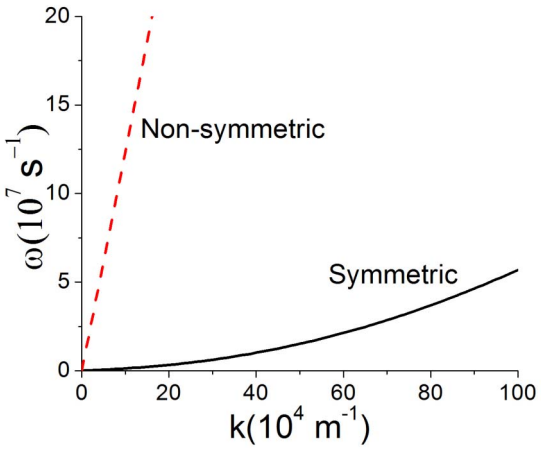

Figure 5 | Dispersion of zero sound as a function of wave vector in the direction of external magnetic field for symmetric and non-symmetric states, respectively. For the non-symmetric state, we choose H = 1 kOe and d = 5 μm.

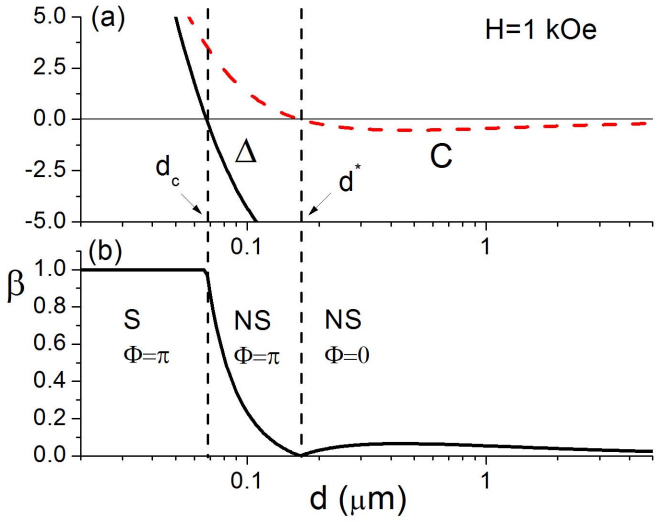

Figure 6 | (a) Criterion for phase transition Δ and interaction coefficient C as a function of thickness d for fixed magnetic field $H = 1$ kOe. (b) The contrast $\beta = \frac{|\Psi|^2_{max} - |\Psi|^2_{min}}{|\Psi|^2_{max} + |\Psi|^2_{min}}$ as a function of thickness d for $H = 1$ kOe. S and NS denote symmetric and non-symmetric state, respectively.

only on film thickness d and magnetic field H. By varying d and H, the contrast can be changed. Specifically, in the symmetric state, $\beta = 1$; in the non-symmetric state, $\beta < 1$; and in the completely non-symmetric state with only one condensate, $\beta = 0$. Therefore, measurement of the contrast for different values of d and H can give complete information on the phase diagram of the system, for comparison with the present theory.

Fig. 6 plots C, Δ and β as functions of the film thickness d at fixed magnetic field $H = 1$ kOe. For small d as H increases the system is in the high-contrast symmetric state. At a larger thickness $d_c = 0.07$ μm, the sign of Δ changes, indicating a transition from the symmetric to the low-contrast non-symmetric state. As d further increases, to $d^* = 0.17$ μm, C changes sign, where the total phase Φ changes from π to 0. Only at this point d^* does the zero-contrast state (with only one condensate) appear. Correspondingly, a characteristic cusp in the contrast β appears near d^*.

To conclude, we have calculated the 4-th order magnon-magnon interactions in the condensate of a film of YIG, including magnon-non-conserving term responsible for the coherence of two condensates. We predict a phase transition from symmetric to non-symmetric state that happens at a reasonable magnetic field > 0.2 kOe in sufficiently thin YIG films $d < 0.1$ μm. We also predict that within the non-symmetric state there is a thickness $d^*(H)$ where the modulation in the observed interference pattern should totally disappear.

Methods

Magnon spectrum. In a YIG film with an in-plane external magnetic field H, the magnon dispersion has been studied extensively[28–30]. At low energies, YIG can be described as a Heisenberg ferromagnet with effective large-spin $S = 14.3$[19,24] on a cubic lattice. The Hamiltonian consists of three parts:

$$\mathcal{H} = -J\sum_{\langle i,j\rangle}\mathbf{S}_i\cdot\mathbf{S}_j + H_D - \gamma H\sum_i S_i^z, \tag{8}$$

the nearest neighbor exchange energy, the dipolar interaction and the Zeeman energy. We take y to be perpendicular to the film and the magnetic field to be in the plane along z. It is convenient to characterize the exchange interaction by the constant $D = 2JSa^2 = 0.24$ eVÅ^2. The dipolar interaction can be calculated using the method indicated in Refs. 20,30. The competition between the dipolar interaction and exchange interaction leads to a magnon spectrum ω_k with minima located at the two points in 2D wave-vector space given by $\mathbf{k} = (0, \pm Q)$ (i.e. along z), with an energy gap Δ_0. For film thickness $d = 5$ μm and magnetic field $H = 1$ kOe, we find $Q = 7.5 \times 10^4$ cm^{-1} and $\Delta_0 = 2.7$ GHz. In the experiment[17] the wave vector Q was found to be about 3.5×10^4 cm^{-1}, i.e. about half the predicted value. The reason for this may be associated with a rather shallow minimum. In such a situation small corrections to our approximate formula can have a large effect on the value of Q. The lowest band of the magnon spectrum can be calculated with the help of the Holstein-Primakoff transformation[32] expressing the spin operator $\mathbf{S}$ in terms of boson operators a and $a^\dagger$.

To second order in a and $a^\dagger$, the Hamiltonian eq.(8) is:

$$\mathcal{H}_0 = \sum_{\mathbf{k}}\left[\mathcal{A}_k a_k^\dagger a_k + \frac{1}{2}\mathcal{B}_k a_k a_{-k} + \frac{1}{2}\mathcal{B}_k^* a_k^\dagger a_{-k}^\dagger\right], \tag{9}$$

with

$$\begin{aligned}\mathcal{A}_k &= \gamma H_0 + Dk^2 + \gamma 2\pi M(1-F_k)\sin^2\theta + \gamma 2\pi M F_k \\ \mathcal{B}_k &= \gamma 2\pi M(1-F_k)\sin^2\theta - \gamma 2\pi M F_k\end{aligned} \tag{10}$$

where $F_k \equiv (1 - e^{-kd})/kd$ and M is the magnetization of the material ($4\pi M = 1.76$ kG). Here, θ is the angle between the 2D wave vector $\mathbf{k}$ and the direction of magnetic field (z). $\mathcal{H}_0$ of eq.(9) is diagonalized by the Bogoliubov transformation $a_k = u_k c_k + v_k c_{-k}^\dagger$ with $u_k = \left(\frac{\mathcal{A}_k + \hbar\omega_k}{2\hbar\omega_k}\right)^{1/2}$ and $v_k = sgn(\mathcal{B}_k)\left(\frac{\mathcal{A}_k - \hbar\omega_k}{2\hbar\omega_k}\right)^{1/2}$, leading to the magnon spectrum:

$$\hbar\omega_k = \left(\mathcal{A}_k^2 - |\mathcal{B}_k|^2\right)^{1/2}. \tag{11}$$

Fig. 1 gives the magnon spectrum along k_z for typical values of thickness d and magnetic field H.

Number of condensed magnons. $N_c = N_Q + N_{-Q}$. Experimentally, the spin lattice relaxation time is of order 1 μs, whereas the magnon-magnon thermalization time is of order 100 ns; the magnons are long-lived enough to equilibrate before decaying, thus making BEC possible[11]. After the thermalization time the pumped magnons go to a quasi-equilibrium state with a non-zero chemical potential μ. The number of pumped magnons $N_p = N(T, \mu) - N(T, 0)$, where $N(T,\mu) = \sum_k \frac{1}{e^{(\omega_k - \mu)/T} - 1}$, is determined by the pumping power and the magnon lifetime. μ is a monotonically increasing function of N_p but cannot exceed the energy gap Δ_0. Therefore, on further increase of pumping some of the pumped magnons fall into the condensate. The equation $N_{pc} = N(T, \Delta_0) - N(T, 0)$ thus defines the critical line of condensation. Since $\Delta_0 \ll T$ and $N_p \ll N(T, 0)$ this equation can be satisfied at a rather high temperature. The total number of condensed particles is[11,31]

$$N_c = N_p - N(T,\Delta_0) + N(T,0) = N(T,\mu) - N(T,\Delta_0). \tag{12}$$

In exactly 2D systems BEC formally does not exist since in the continuum approximation the sum in $N(T, \mu)$ diverges. However, for strong enough pumping the chemical potential approaches exponentially close to the energy gap: $\Delta_0 - \mu \approx \Delta_0 \exp(-N_p/N_0)$, where $N_0 = VTm/\hbar^2$. For $N_p/N_0 > \ln(T/\Delta_0)$ all pumped magnons occupy only one or two states $\pm Q$.

Eq.(12) determines only the total number of particles in the condensate. The distribution of the condensate particles between the two minima remains undetermined in the quadratic approximation. To resolve this issue it was necessary to consider the fourth order terms in the Holstein-Primakoff expansion of the exchange and dipolar energy. Terms of third order in this expansion occur due to the dipolar interaction, but they vanish for the condensate values of momentum $(0, \pm Q)$ since in the third order the total momentum cannot be zero.

Zero sound. Here we provide details in calculating the zero sound spectrum. Let us consider small deviations from the static symmetric solution $n_Q = n_{-Q} = n_c/2$, $\phi_+ = \pi - \phi_- = 0$ so that $n_{\pm Q} = n_c/2 + \delta n_\pm$ with $\delta n_+ = -\delta n_- = \delta n/2$ and $\delta\phi_+ = -\delta\phi_- = \delta\phi/2$. Then

$$\begin{aligned}E = \int dr\Big(&\frac{\hbar^2}{2m}\left(|\nabla\Psi_+|^2 + |\nabla\Psi_-|^2\right) + AV\left(|\Psi_+|^4 + |\Psi_-|^4\right) \\ &+ 2BV|\Psi_+|^2|\Psi_-|^2 + CV\left(\Psi_+\Psi_- + \Psi_+^*\Psi_-^*\right)\left(|\Psi_+|^2 + |\Psi_-|^2\right)\Big),\end{aligned}$$

On linearizing, the energy reads:

$$E = \int dr\left(\frac{\hbar^2}{4mn_c}|\nabla\delta n|^2 + \frac{\hbar^2 n_c}{4m}|\nabla\delta\phi|^2 + \frac{\Delta V}{2}\delta n^2\right). \tag{13}$$

Using the commutation relation $[\delta\phi, \delta n] = i$, and the equation of motion $i\hbar\dot{\Delta\phi} = [\Delta\phi, H]$, we obtain:

$$\hbar\frac{\partial\delta\phi}{\partial t} = -\frac{\hbar^2}{2mn_c}\nabla^2\delta n + \Delta V\delta n, \tag{14}$$

$$\hbar\frac{\partial\delta n}{\partial t} = \frac{\hbar^2}{2m}n_c\nabla^2\delta\phi. \tag{15}$$

Taking Fourier transforms of the above two equations in coordinate and time, one arrives at dispersion relations Eq.(6).

1. Kapitza, P. Viscosity of Liquid Helium Below the λ-point. *Nature* **141**, 74–74 (1938).

2. Allen, J. F. & Misener, A. D. Flow of Liquid Helium II. *Nature* **141**, 75–75 (1938).
3. Anderson, M. H., Ensher, J. R., Matthews, M. R., Wieman, C. E. & Cornell, E. A. Observation of Bose-Einstein Condensation in a Dilute Atomic Vapor. *Science* **269**, 198–201 (1995).
4. Davis, K. B. *et al.* Bose-Einstein Condensation in a Gas of Sodium Atoms. *Phys. Rev. Lett.* **75**, 3969–3973 (1995).
5. Klaers, J., Schmitt, J., Vewinger, F. & Weitz, M. Bose-Einstein Condensation of Photons in an Optical Microcavity. *Nature* **468**, 545–548 (2010).
6. Butov, L. V. *et al.* Stimulated Scattering of Indirect Excitons in Coupled Quantum Wells: Signature of a Degenerate Bose-Gas of Excitons. *Phys. Rev. Lett.* **86**, 5608–5611 (2011).
7. Kasprzak, J. *et al.* Bose-Einstein Condensation of Exciton Polaritons. *Nature* **443**, 409–414(2006).
8. Balili, R., Hartwell, V., Snoke, D., Pfeiffer, L. & West, K. Bose-Einstein Condensation of Microcavity Polaritons in a Trap. *Science* **316**, 1007–1010 (2007).
9. Amo, A. *et al.* Collective Fluid Dynamics of a Polariton Condensate in a Semiconductor Microcavity. *Nature* **457**, 291–295 (2009).
10. Bunkov Yu, M. & Volovik, G. E. Bose-Einstein Condensation of Magnons in Superfluid ^{3}He. *J. Low Temp. Phys.* **150**, 135–144 (2008).
11. Demokritov, S. O. *et al.* Bose-Einstein Condensation of Quasi-equilibrium Magnons at Room Temperature under Pumping. *Nature* **443**, 430–433 (2006).
12. Dzyapko, O., Demidov, V. E., Demokritov, S. O., Melkov, G. A. & Slavin, A. N. Direct Observation of Bose-Einstein Condensation in a Parametrically Driven Gas of Magnons. *New J. Phys.* **9**, 64 (2007).
13. Demidov, V. E., Dzyapko, O., Demokritov, S. O., Melkov, G. A. & Slavin, A. N. Thermalization of a Parametrically Driven Magnon Gas Leading to Bose-Einstein Condenstate. *Phys. Rev. Lett.* **99**, 037205 (2007).
14. Demidov, V. E., Dzyapko, O., Demokritov, S. O., Melkov, G. A. & Slavin, A. N. Observation of Spontaneous Coherence in Bose-Einstein Condensate of Magnons. *Phys. Rev. Lett.* **100**, 047205 (2008).
15. Demidov, V. E. *et al.* Magnon Kinetics and Bose-Einstein Condensation Studied in Phase Space. *Phys. Rev. Lett.* **101**, 257201 (2008).
16. Dzyapko, O. *et al.* Excitation of Two Spatially Separated Bose-Einstein Condensate of Magnons. *Phys. Rev. B* **80**, 060410 (R) (2009).
17. Nowik-Boltyk, P., Dzyapko, O., Demidov, V. E., Berloff, N. G. & Demokritov, S. O. Spatially Nonuniform Ground State and Quantized Vortices in a Two-component Bose-Einstein Condensate of Magnons. *Sci. Rep.* **2**, 482 (2012).
18. Leggett, A. J. Bose-Einstein Condensation in the Alkali Gases: Some Fundamental Concepts. *Rev. Mod. Phys.* **73**, 307–356 (2003).The author notes that a system with multiple condensates possess what is sometimes called "fragmentation." In the present case the fragmentation is in momentum space; for inhomogeneous systems fragmentation can occur in real space.
19. Tupitsyn, I. S., Stamp, P. C. E. & Burin, A. L. Stability of Bose-Einstein Condensates of Hot Magnons in Yttrium Iron Garnet Films. *Phys. Rev. Lett.* **100**, 257202 (2008).
20. Rezende, S. M. Theory of Coherence in Bose-Einstein Condensation Phenomena in a Microwave Driven Interacting Magnon Gas. *Phys. Rev. B* **79**, 174411 (2009).
21. Rezende, S. M. Crossover Behavior in the Phase Transition of the Bose-Einstein Condensation in a Microwave-Driven Magnon Gas. *Phys. Rev. B* **80**, 092409 (2009).
22. Rezende, S. M. Wave Function of a Microwave-Driven Bose-Einstein Magnon Condensate. *Phys. Rev. B* **81**, 020414(R) (2010).
23. Malomed, B. A., Dzyapko, O., Demidov, V. E. & Demokritov, S. O. Ginzburg-Landau Model of Bose-Einstein Condensation of Magnons. *Phys. Rev. B* **81**, 024418 (2010).
24. Troncoso, R. E. & Nunez, A. S. Dynamics and Spontaneous Coherence of Magnons in Ferromagnetic Thin Films. *J. Phys.: Condens. Matter* **24**, 036006 (2012).
25. Cherepanov, V., Kolokolov, I. & L'vov, V. The Saga of YIG: Spectra, Thermodynamics, Interaction and Relaxation of Magnons in a Complex Magnet. *Phys. Rep.* **229**, 81–144 (1993).
26. Slavin, A. N. & Rojdestvensky, I. V. "Bright" and "Dark" Spin-Wave Envelope Solitons in Tangentially Magnetized Yttrium-Iron Garnet Films. *IEEE Transactions on Magnetics* **30**, 37–45 (1994).
27. Krivosik, P. & Patton, C. E. Hamiltonian Formulation of Nonlinear Spin-Wave Dynamics: Theory and Applications. *Phys. Rev. B* **82**, 184428 (2010).
28. Damon, R. W. & Eshbach, J. R. Magnetostatic Modes of a Ferromagnet Slab. *J. Phys. Chem. Solids* **19**, 308–320 (1961).
29. Sparks, M. Ferromagnetic Resonance in Thin Films. I. Theory of Normal-Mode Frequencies. *Phys. Rev. B* **1**, 3831–3856 (1970).
30. Kalinikos, B. A. Excitation of Propagating Spin Waves in Ferromagnetic Films. *IEEE Proc., Part H: Microwaves, Opt. Antennas* **127**, 4–10 (1980).
31. Bunkov, Y. M. & Volovik, G. E. Spin Superfluidity and Magnon BEC. arXiv: 1003.4889v1.
32. Madelung, O. *Introduction to Solid-State Theory* (Springer, Berlin, 2008).

Acknowledgment

This work was partly supported by the grant of DOE DE-FG02-06ER46278. We are thankful to H. Schulte attracting our attention to the experimental work[17] and to S. M. Rezende, I.S. Tupitsyn and V. E. Demidov for useful discussion.

Author contributions

All authors contributed to the theoretical analysis and the preparation of the manuscript.

Additional information

Competing financial interests: The authors declare no competing financial interests.

How to cite this article: Li, F., Saslow, W.M. & Pokrovsky, V.L. Phase Diagram for Magnon Condensate in Yttrium Iron Garnet film. *Sci. Rep.* **3**, 1372; DOI:10.1038/srep01372 (2013).